Short Note

2-Bromo-3-((1-(7-chloroquinolin-4-yl)-1H-1,2,3-triazol-4-yl)-methoxy)-benzaldehyde

Xiaoyun Yun [1,2] (ID)**, Yuhan Xie** [3]**, Jerome P. L. Ng** [1,2]**, Betty Yuen Kwan Law** [1,2]**, Vincent Kam Wai Wong** [1,2,*] **and Paolo Coghi** [3,*]

[1]   Dr. Neher's Biophysics Laboratory for Innovative Drug Discovery, State Key Laboratory of Quality Research in Chinese Medicine, Macau University of Science and Technology, Macau 999078, China; yunxiaoyunjudy@163.com (X.Y.); plng@must.edu.mo (J.P.L.N.); yklaw@must.edu.mo (B.Y.K.L.)

[2]   State Key Laboratory of Quality Research in Chinese Medicine, Macau University of Science and Technology, Macau 999078, China

[3]   School of Pharmacy, Macau University of Science and Technology, Macau 999078, China; 19098533pa11002@student.must.edu.mo

*   Correspondence: bowaiwong@gmail.com (V.K.W.W.); coghips@must.edu.mo (P.C.); Tel.: +853-8897-2408 (V.K.W.W.)

Abstract: The 1,2,3-triazole ring system can be easily obtained by copper-catalyzed click reaction of azides with alkynes. 1,2,3-Triazole exhibits a myriad of biological activities, including antimalarial, antibacterial, and antiviral activities. We herein reported the synthesis of quinoline-based [1,2,3]-hybrid via Cu(I)-catalyzed click reaction of 4-azido-7-chloroquinoline with alkyne derivative of 2-bromobenzaldehyde. The compound was fully characterized by proton nuclear magnetic resonance (^{1}H-NMR), carbon-13 nuclear magnetic resonance (^{13}C-NMR), heteronuclear single quantum coherence (HSQC), ultraviolet (UV), and high-resolution mass spectroscopies (HRMS). This compound was screened in vitro against two different normal cell lines. Preliminary studies attempted to evaluate its interaction with Delta RBD of spike protein of SARS-CoV-2 by bio-layer interferometry. Finally, the drug-likeness of the compound was also investigated by predicting its pharmacokinetic properties.

Keywords: 1,2,3-triazole; bio-layer interferometry; RBD; SARS-CoV-2

1. Introduction

In December 2019, a novel pneumonia emerged in Wuhan, caused by a previously unknown pathogen. This pathogen was later identified as a novel coronavirus (initially named 2019-nCoV and now called SARS-CoV-2, which has a similar infection to severe acute respiratory syndrome CoV (SARS-CoV-1) discovered in 2003 [1].

In early in vitro studies, antimalarial chloroquine (Figure 1a) was found to counteract COVID-19 infection at a low-micromolar concentration, with a half-maximal effective concentration (EC_{50}) of 1.13 μM and a half-cytotoxic concentration (CC_{50}) greater than 100 μM [2,3].

The 7-chloroquinoline moiety, a pharmacophore of several established antimalarial drugs, such as chloroquine (Figure 1a) [1], has been recently recognized as a potential anti-cancer agent, as well as a chemosensitizer, when used in combination with anti-cancer drugs [4].

Intensive drug discovery efforts for developing new antimalarial/antiviral drugs or modifying existing agents are ongoing (Figure 1b) [5]. Molecular hybridization is a well-established strategy that combines two compounds or their moieties into a new, single hybrid molecule [6].

Considering the physicochemical and pharmacological features of known scaffolds, it is possible to expand drug libraries of homologous molecular hybrids through the fusion (usually via a covalent linker) of two drugs [7].

Therefore, a well-known scaffold, 1,2,3-triazole [8], appears frequently in medicinal compounds, and many covalently linked triazole hybrids exhibit diverse biological activities, such as antibacterial [9], antitubercular [10], anti-viral [5], antimalarial [11], and anti-inflammatory effects (Figure 1c–f).
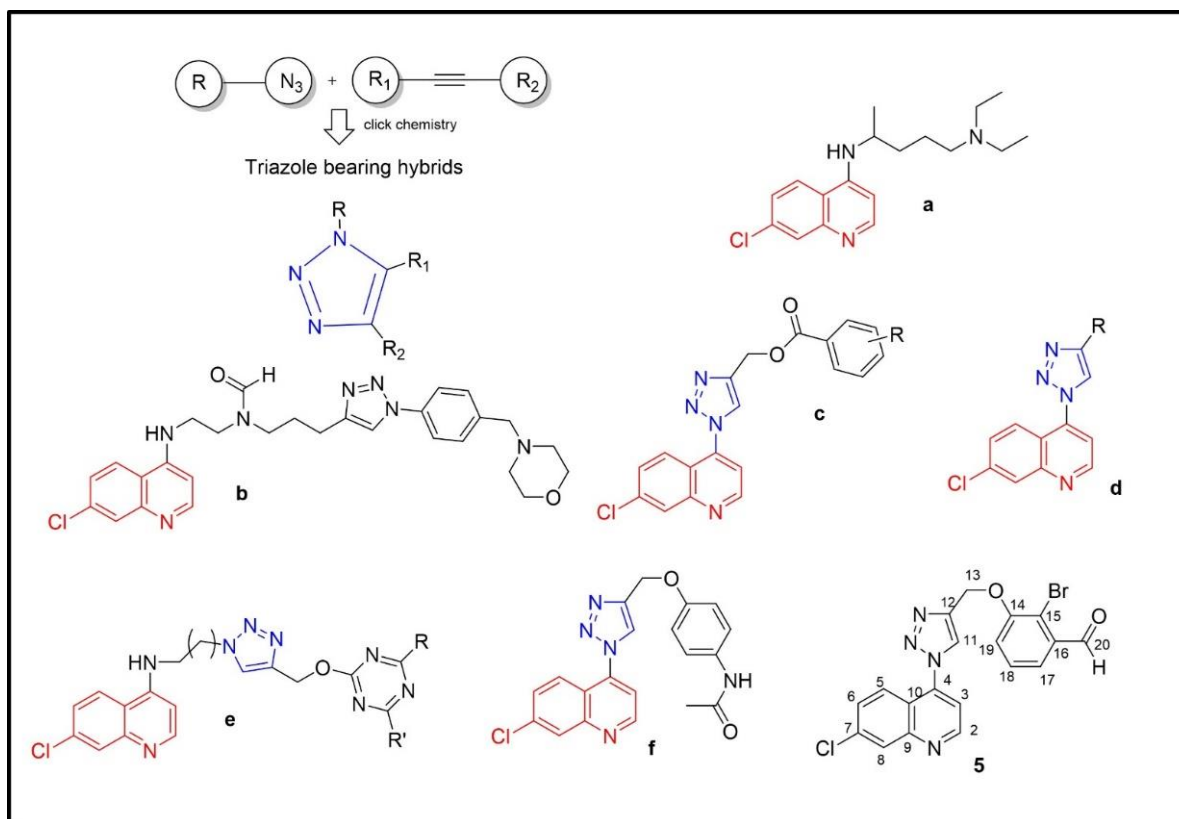

Figure 1. Clinically approved quinoline (red) and 1,2,3-triazole (blue) containing drugs (some structures of quinolone- and triazole-based hybrids reported in the literature (**a**–**f**) [9–14]); and the structure of the compound (cyan, **5**) reported in this paper. Square: synthesis of 1,2,3-triazoles using click chemistry.

Previously, we reported the synthesis of a novel 4-amino-7-chloroquinoline-based 1,2,3-triazole hybrid **f** by Cu(I)-catalyzed azide-alkyne cycloaddition (click chemistry) [12]. Recently, a library of 1,2,3-triazoles 4-aminoquinoline-benzoxaborole derivatives was synthesized [13], and our recent interest in boron derivatives [14] advanced further studies on similar derivatives.

In this study, analog compound **5** was synthesized and characterized using NMR, MS and UV spectra. The cytotoxicity of 5 was also evaluated against different cell lines and evaluated for interaction of the RBD spike protein of SARS-CoV-2.

2. Results and Discussion

The synthetic route of the triazole hybrid compound, 2-bromo-4-((1-(7-chloroquinolin-4-yl)-1H-1,2,3-triazol-4-yl)-methoxy)-benzaldehyde **5**, started from the preparation of precursors, 4-azido-7-chloroquinoline 2 and *O*-acetylenic derivative **4** (Scheme 1).
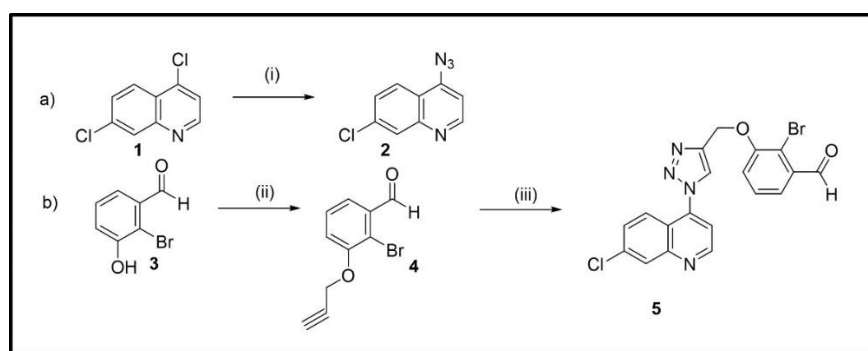
Scheme 1. (**a**) Synthesis of 4-azido-7-chloro-quinoline (i) NaN$_3$, DMF; (**b**) Synthesis of 2-bromo-3-((1-(7-chloroquinolin-4-yl)-1H-1,2,3-triazol-4-yl)-methoxy)-benzaldehyde (ii) propargyl bromide, DMF, K$_2$CO$_3$; (iii) **2**, CuSO$_4$, ascorbic acid, *t*BuOH/water (1:1).

Similar to the protocol reported by de Souza et al. [15], quinoline 2 was prepared by the reaction of 4,7-dichloroquinoline **1** with NaN$_3$ (2 equiv.) in anhydrous DMF at 65 °C for 6 h (Scheme 1a). The crude product was purified by recrystallization from CH$_2$Cl$_2$/hexane to afford 2 in 78% yield.

The other cycloaddition partner, acetylenic intermediate 4, was generated by *O*-alkylation of 2-bromo-3-hydroxybenzaldehyde **3** with propargyl bromide (1.5 equiv.) and anhydrous K$_2$CO$_3$ in anhydrous DMF with a good yield (82%) after recrystallization from CH$_2$Cl$_2$/hexane (Scheme 1b).

Finally, the hybrid compound **5** was then furnished by using a modified protocol of click reaction reported by Fokin et al. [16]. Equimolars of quinoline **2** and acetylene **4** in *t*BuOH/water (1:1) were subjected to sequential additions of sodium ascorbate (0.4 equiv.) and CuSO$_4$ (20 mol%) (Scheme 1b). After stirring at 65 °C for 24 h, compound **5** was isolated by column chromatography in a high yield (77%).

The structure of **5** was determined by ^{1}H and ^{13}C-NMR spectra (Supplementary Materials, Figures S3 and S4). The ^{1}H-NMR spectrum showed a singlet at 5.53 ppm corresponding to C13-methylene group and a singlet at 10.30 ppm corresponding to the C20-aldehydic proton.

For the ^{13}C-NMR signals, the disappearance of the characteristic peaks of acetylenic group at 77.4 and 76.7 ppm, and the appearance of the C-13 methylene signal at 61.6 ppm and C-11 vinylic signal at 126.6 ppm were the proposed relevant characteristics to recognize the synthesis of a triazole moiety.

Heteronuclear single quantum coherence spectroscopy (HSQC) was also used to assign ^{13}C signals of compound **5**, as shown in Table S1 (see Supplementary Materials for 2D spectra, Figures S5 and S6).

The UV spectrum of compound **5** showed an absorption peak at 233 nm [11–13] and a broad absorption peak from 275 nm to 325 nm (*n*→π transition) (Supplementary Materials, Figure S7).

The HRMS of **5** was also obtained for further characterization, validating the proposed structure determined by NMR spectra (Supplementary Materials, Figure S8).

On the other hand, target compound **5** showed a low cytotoxicity by evaluating its in vitro cytotoxic activities against liver and lung normal cells (LO$_2$ and BEAS-2B) (IC$_{50}$ values > 100 and 55 μM, respectively, Supplementary Materials, Figure S9).

In addition, compound **5** was assessed by predicting its physicochemical properties and oral bioavailability. From the calculated physicochemical properties (Supplementary Materials, Table S2), compound **5** did not violate any Lipinski's rules [17], indicating its drug-like character and a good chance for oral administration.

This finding corroborates the results of gastrointestinal absorption from SwissADME in which compound was predicted by BOILED-Egg model with high probability to passively permeate through the blood–brain barrier absorption [18] (Figure S10). Compound **5** was predicted to be orally bioavailable and absorbed in human intestine from admetSAR 2 [19].

The binding of compound **5** with Delta RBD of spike protein of SARS-CoV-2 was then tested in vitro by bio-layer interferometry (BLI), a label-free technology for measuring biomolecular interactions. This experiment is based on the immobilization of the target protein on the biosensor exposed to different ligand concentrations, thus monitoring the real-time association and dissociation events. BLI also provides the calculation of kinetic parameters, such as association rate (k_{on}) and dissociation rate (k_{dis}), as well as of dissociation constant (K_D). This technique was recently adopted to screen RBD ligands in combination with virtual screening [20]. As shown in Figure S11 of the Supplementary Materials, the results of BLI conducted on synthesized compound demonstrated a poor affinity with RBD spike of SARS-CoV-2 (delta variant), with a modest correlation value.

3. Materials and Methods

3.1. Chemistry

Silica gel (FCP 230–400 mesh) was used for column chromatography. Thin-layer chromatography was carried out on E. Merck precoated silica gel 60 F_{254} plates and visualized with phosphomolybdic acid, iodine, or a UV-visible lamp.

All chemicals were purchased from Bide Pharmatech., Ltd. (Shanghai, China) and J & K scientific (Hong Kong, China). ^{1}H-NMR and ^{13}C-NMR spectra were collected in $CDCl_3$ at 25 °C on a Bruker Ascend®-600 NMR spectrometer (600 MHz for ^{1}H and 150 MHz for ^{13}C). All chemical shifts were reported in the standard δ notation of parts per million using the peak of residual proton signals of $CDCl_3$ or DMSO-d_6 as an internal reference ($CDCl_3$, δ_C 77.2 ppm, δ_H 7.26 ppm; DMSO-d_6, δ_C 39.5 ppm, δ_H 2.50 ppm). High resolution mass spectra (HRMS) were measured using electrospray ionization (ESI). The measurements were done in a positive ion mode (interface capillary voltage 4500 V); the mass ratio was from *m/z* 50 to 3000 Da; external/internal calibration was done with electrospray calibration solution.

HRMS analyses were performed using an Agilent 6230 electrospray ionization (ESI) time-of-flight (TOF) mass spectrometer with Agilent C18 column (4.6 mm × 150 mm, 3.5 μm). The mobile phase was isocratic (water + 0.01% TFA; CH_3CN) at a flow rate of 0.35 mL/min. The peaks were determined at 254 nm under UV.

UV analysis was performed by a Shimadzu UV–2600 with 1 cm quartz cell and a slit width of 2.0 nm. The analysis was carried out using wavelength in the range of 200–400 nm.

3.1.1. Synthesis of 4-Azido-7-chloroquinoline (**2**)

4,7-Dichloroquinoline **1** (1.98 g, 10 mmol) was dissolved in 5 mL anhydrous DMF. NaN_3 (1.3 g, 20 mmol) was then added in one portion, and the resulting mixture was stirred at 65 °C for 6 h, whereupon TLC indicated the completion of the reaction. The reaction mixture was then allowed to cool to room temperature, after which it was diluted with 100 mL CH_2Cl_2, washed with water (3 × 30 mL), dried over anhydrous Na_2SO_4, and evaporated to dryness. The resulting residue was recrystallized from a 1:1 mixture of CH_2Cl_2/hexane to yield the final pure product **2** as a colorless, needle-like crystal in 78% yield.

R_f (CH_2Cl_2) 0.5; δ_H (600 MHz, $CDCl_3$) 8.82 (1H, d, *J* = 4.9 Hz, H-2), 8.09 (1H, d, *J* = 2.4 Hz, H-8), 8.01 (1H, d, *J* 9.3, H-5), 7.49 (1H, dd, *J* 2.4 and 9.3, H-6) 7.12 (1H, d, *J* 4.9, H-3) ppm; δ_C (150 MHz, $CDCl_3$) 150.9, 149.1, 146.8, 136.9, 127.9, 123.8, 119.9, 108.7 ppm. The spectral characteristics are consistent with those of **2** in the literature [20].

3.1.2. Synthesis of 2-Bromo-3-(prop-2-yn-1-yloxy) benzaldehyde (**4**)

2-Bromo-3-hydroxybenzaldehyde **3** (2.61 g, 13 mmol) was dissolved in 10 mL of anhydrous DMF. Anhydrous K_2CO_3 (2.7 g, 19.5 mmol) was then added to the solution, and the mixture was stirred at 30 °C for 30 min. Propargyl bromide (3-bromopropyne, 2.2 mL, 19.5 mmol) was then added slowly to the reaction mixture, and subsequently stirred at 30 °C for 6 h upon which TLC indicated completion of the reaction. The reaction mixture was diluted with water (50 mL) and extracted with ethyl acetate (3 × 50 mL). These extracts were then combined, washed with water (2 × 50 mL), dried over anhydrous

Na_2SO_4 and evaporated in vacuo to yield the product residue that was then recrystallized from CH_2Cl_2/hexane 1:1 mixture to yield the compound 4 in 82% yield (2.54 g). Mp 90 °C; R_f (CH_2Cl_2) 0.9; δ_H (600 MHz, $CDCl_3$) 2.58 (H, s), 4.84 (2H, s, CH_2), 7.30 (H, dd, $J = 1.33$ and 8.24 Hz, H_{Ar}), 7.40 (1H, t, H_{Ar}), 7.58 (1H, dd, $J = 1.4$ and 7.9 Hz, H_{Ar}), 10.44 (CHO, s) ppm; δ_C (150 MHz, $CDCl_3$) 57.4, 76.7, 77.4, 117.8, 119.2, 122.5, 128.1, 135.0, 154.4, 192.4 ppm; HRMS-ESI m/z 236.9556 [M–H]$^-$ (calcd. for $C_{10}H_7BrO_2$, m/z 236.9557)

3.1.3. Synthesis of 2-Bromo-3-((1-(7-chloroquinolin-4-yl)-1H-1,2,3-triazol-4-yl)-methoxy)-benzaldehyde (5)

The *O*-acetylenic derivative 4 (239 mg, 1 mmol) and azide **2** (204 mg, 1 mmol) were dissolved in 5 mL *t*BuOH/water (1:1) and, while stirring at 65 °C, 1 M sodium ascorbate (0.4 mL, 0.4 mmol) and 1 M $CuSO_4$ (0.2 mL, 20 mol%) were added sequentially, in that order. The reaction mixture was then stirred at 65 °C for 24 h. The crude product was then precipitated out by slowly adding cold water to the reaction mixture, after which it was filtered, washed with water, air dried and purified by silica column chromatography (eluents: from EtOAc/Hex 3:7 to 5% MeOH in EtOAc) in yield 77% (341 mg). Mp 140 °C; R_f (CH_2Cl_2) 0.2; δ_H (600 MHz, DMSO-d_6) 5.53 (2H, s, CH_2-O), 7.49 (1H, dd, $J = 1.3$ and 7.6 Hz, H-17), 7.58 (1H, t, $J = 9$ Hz, H-18), 7.75 (1H, dd, $J = 1.3$ and 8.2 Hz, H-19), 7.81 (1H, dd, $J = 2.3$ and 9.1 Hz, H-6), 7.90 (1H, d, $J = 4.6$ Hz, H-3), 7.99 (1H, d, $J = 9.1$ Hz, H-5), 8.31 (1H, d, $J = 2.1$ H-8), 9.02 (1H, s, H-11), 9.18 (1H, d, $J = 4.6$ Hz, H-2), 10.30 (1H, s, C*H*O) ppm; δ_C (150 MHz, DMSO-d_6) 61.6 (C-13), 115.4 (C-15), 116.6 (C-3), 119.1, 119.7, 121.3, 124.7 (C-5), 126.6 (C-11), 127.5, 128.3 (C-6), 128.5, 133.9 (C-16), 134.8 (C-4), 139.7, 142.3, 148.8 (C-9), 151.7 (C-2), 154.2 (C-14), 191.3 (CO) ppm; HRMS-ESI m/z 442.9917 [M + H]$^+$ (calcd. for $C_{19}H_{12}BrClN_4O_2$, m/z 442.9905); UV (CH_2Cl_2) peaks 221, 233, 284 and 312 nm.

3.2. Biological Studies

3.2.1. Cytotoxicity Drug Assay

Compound **5** was dissolved in DMSO at a final concentration of 100 mM and stored at -20 °C before use. Cytotoxicity was assessed by using the 3-(4,5-dimethylthiazole-2yl)-2,5-diphenyltetrazolium bromide (MTT) (5 mg/mL) assay as previously described [21]. Briefly, 4×10^3 cells per well were seeded in 96-well plates before drug treatments. After overnight cell culture, the cells were then exposed to different concentration of selected compounds (0.8–200 µM) for 48 h. Cells without drug treatment were used as control. Subsequently, 10 µL of 5 mg/mL MTT solution was added to each well and incubated at 37 °C for 4 h followed by addition of 100 µL solubilization buffer (10 mM HCl in solution of 10% of SDS) and overnight incubation. A_{570} nm was then determined in each well on the next day. The percentage of cell viability was calculated using the following formula: Cell viability (%) = $A_{treated}/A_{control} \times 100$. A representative graph of at least three independent experiments was shown in the Supplementary Materials, Figure S9.

3.2.2. Biolayer Interferometry Assay

Purified SARS-CoV-2 RBD peptide (Sino Biological, Beijing, China) were conjugated with biotin using EZ-Link™ Sulfo-NHS-Biotin (Genemore, Suzhou, China) according to the manufacturer's protocol. Then, the biotinylated SARS-CoV-2 RBD peptide were immobilized onto Super Streptavidin (SSA) biosensors (Fortebio, San Francisco, CA, USA). SARS-CoV-2 RBD peptide (Sino Biological, Beijing, China) was immobilized onto the biosensor coated with nickel-nitrilotriacetic acid (Ni-NTA, Fortebio, San Francisco United States). After the setup of the baseline with PBS containing 2% DMSO (Sigma-aldrich, St. Louis, MA, USA), biosensor tips were immersed into the wells containing serial dilutions of SARS-CoV-2 RBD peptide for 180 s of association, followed by a dissociation step of 180 s. The KD value was calculated by using a 1:1 binding model in Data Analysis Software 9.0 (Fortebio, San Francisco, CA, USA). Compounds were serially diluted from 200 µM to 6.25 µM with PBS (Figure S11 of the Supplementary Materials).

4. Conclusions

The synthesis of a triazole-based quinoline was presented. The synthesized compound was characterized by using NMR, mass and UV spectrometry. The cytotoxicity and drug-likeness of the compound were also determined by MTT assay and computations respectively. Finally, the compound was investigated for its interaction with Delta RBD of spike protein of SARS-CoV-2 by bio-layer interferometry.

Supplementary Materials: The following are available online, Figure S1: ^{1}H-NMR compound **4**, Figure S2: ^{13}C-NMR compound **4**, Figure S3: ^{1}H-NMR compound **5**, Figure S4: ^{13}C-NMR compound **5**, Figures S5 and S6: HSQC compound **5**, Figure S7: UV spectrum; Figure S8: HRMS of **4** and **5**, Figure S9: cytotoxicity results, Table S1: ^{1}H and ^{13}C-nuclear magnetic spectroscopy (NMR) chemical shifts, Table S2: Physicochemical properties of **5** calculated by SwissADME, Figure S10: BOILED-Egg graph, Figure S11: Biolayer interferometry of compound **5**. References [18,22,23] are cited in the supplementary materials.

Author Contributions: Conceptualization, P.C.; methodology, P.C. and J.P.L.N.; investigation, X.Y. and Y.X.; data curation, J.P.L.N. and B.Y.K.L.; writing—original draft preparation, J.P.L.N. and P.C.; writing—review and editing, J.P.L.N. and V.K.W.W.; supervision, P.C. and V.K.W.W.; project administration, P.C.; funding acquisition, P.C. All authors have read and agreed to the published version of the manuscript.

Institutional Review Board Statement: Not applicable.

Informed Consent Statement: Not applicable.

Data Availability Statement: Data is contained within the article and Supplementary Materials.

Conflicts of Interest: The authors declare no conflict of interest.

References

1. Huang, C.; Wang, Y.; Li, X.; Ren, L.; Zhao, J.; Hu, Y.; Zhang, L.; Fan, G.; Xu, J.; Gu, X.; et al. Clinical features of patients infected with 2019 novel coronavirus in Wuhan, China. *Lancet* **2020**, *395*, 497–506. [CrossRef]
2. Colson, P.; Rolain, J.M.; Raoult, D. Chloroquine for the 2019 novel coronavirus SARS-CoV-2. *Int. J. Antimicrob. Agents* **2020**, *55*, 105923. [CrossRef] [PubMed]
3. Wang, M.; Cao, R.; Zhang, L.; Yang, X.; Liu, J.; Xu, M.; Shi, Z.; Hu, Z.; Zhong, W.; Xiao, G. Remdesivir and chloroquine effectively inhibit the recently emerged novel coronavirus (2019-nCoV) in vitro. *Cell Res.* **2020**, *30*, 269–271. [CrossRef] [PubMed]
4. Sasaki, K.; Tsuno, N.H.; Sunami, E.; Tsurita, G.; Kawai, K.; Okaji, Y.; Nishikawa, T.; Shuno, Y.; Hongo, K.; Hiyoshi, M.; et al. Chloroquine potentiates the anti-cancer effect of 5-fluorouracil on colon cancer cells. *BMC Cancer* **2010**, *10*, 370. [CrossRef]
5. Herrmann, L.; Hahn, F.; Wangen, C.; Marschall, M.; Tsogoeva, S.B. Anti-SARS-CoV-2 Inhibitory Profile of New Quinoline Compounds in Cell Culture-Based Infection Models. *Chem. Eur. J.* **2022**, *28*, e202103861. [CrossRef] [PubMed]
6. Harrison, J.R.; Brand, S.; Smith, V.; Robinson, D.A.; Thompson, S.; Smith, A.; Davies, K.; Mok, N.; Torrie, L.S.; Collie, I.; et al. A Molecular Hybridization Approach for the Design of Potent, Highly Selective, and Brain-Penetrant N-Myristoyltransferase Inhibitors. *J. Med. Chem.* **2018**, *61*, 8374–8389. [CrossRef]
7. Ivasiv, V.; Albertini, C.; Gonçalves, A.E.; Rossi, M.; Bolognesi, M.L. Molecular Hybridization as a Tool for Designing Multitarget Drug Candidates for Complex Diseases. *Curr. Top. Med. Chem.* **2019**, *19*, 1694–1711. [CrossRef]
8. Bozorov, K.; Zhao, J.; Aisa, H.A. 1,2,3-Triazole-containing hybrids as leads in medicinal chemistry: A recent overview. *Bioorg. Med. Chem.* **2019**, *27*, 3511–3531. [CrossRef]
9. Demaray, J.A.; Thuener, J.E.; Dawson, M.N.; Sucheck, S.J. Synthesis of triazole-oxazolidinones via a one-pot reaction and evaluation of their antimicrobial activity. *Bioorg. Med. Chem. Lett.* **2008**, *18*, 4868–4871. [CrossRef]
10. Tripathi, R.P.; Yadav, A.K.; Ajay, A.; Bisht, S.S.; Chaturvedi, V.; Sinha, S.K. Application of Huisgen (3 + 2) cycloaddition reaction: Synthesis of 1-(2,3-dihydrobenzofuran-2-yl-methyl [1,2,3]-triazoles and their antitubercular evaluations. *Eur. J. Med. Chem.* **2010**, *45*, 142–148. [CrossRef]
11. Guanti, E.M.; Ncokazi, K.; Egan, T.J.; Gut, J.; Rosenthal, P.J.; Smith, P.J.; Chibale, K. Design, synthesis and in vitro antimalarial evaluation of triazole-linked chalcone and dienone hybrid compounds. *Bioorg. Med. Chem.* **2010**, *18*, 8243–8256. [CrossRef] [PubMed]
12. Coghi, P.; Ng, J.P.L.; Nasim, A.A.; Wong, V.K.W. *N*-[7-Chloro-4-[4-(phenoxymethyl)-1*H*-1,2,3-triazol-1-yl] quinoline]-acetamide. *Molbank* **2021**, *2021*, M1213. [CrossRef]

13. Saini, A.; Kumar, S.; Raj, R.; Chowdhary, S.; Gendrot, M.; Mosnier, J.; Fonta, I.; Pradines, B.; Kumar, V. Synthesis and antiplasmodial evaluation of 1H-1,2,3-triazole grafted 4-aminoquinoline-benzoxaborole hybrids and benzoxaborole analogues. *Bioorg. Chem.* **2021**, *109*, 104733. [CrossRef] [PubMed]

14. Coghi, P.S.; Zhu, Y.; Xie, H.; Hosmane, N.S.; Zhang, Y. Organoboron Compounds: Effective Antibacterial and Antiparasitic Agents. *Molecules* **2021**, *26*, 3309. [CrossRef] [PubMed]

15. De Souza, M.V.; Pais, K.C.; Kaiser, C.R.; Peralta, M.A.; de L. Ferreira, M.; Lourenço, M.C. Synthesis and in vitro antitubercular activity of a series of quinoline derivatives. *Bioorg. Med. Chem.* **2009**, *17*, 1474–1480. [CrossRef]

16. Feldman, A.K.; Colasson, B.; Fokin, V.V. One-Pot Synthesis of 1,4-Disubstitued 1,2,3- Triazole from In Situ Generated Azides. *Org. Lett.* **2004**, *6*, 3897–3899. [CrossRef]

17. Lipinski, C.A. Drug-like properties and the causes of poor solubility and poor permeability. *J. Pharmacol. Toxicol. Methods* **2000**, *44*, 235–249. [CrossRef]

18. Daina, A.; Zoete, V.A. Boiled-egg to predict gastrointestinal absorption and brain penetration of small molecules. *ChemMedChem* **2016**, *11*, 1117–1121. [CrossRef]

19. Yang, H.; Lou, C.; Sun, L.; Li, J.; Cai, Y.; Wang, Z.; Li, W.; Liu, G.; Tang, Y. AdmetSAR 2.0: Web-service for prediction and optimization of chemical ADMET properties. *Bioinformatics* **2018**, *35*, 1067–1069. [CrossRef]

20. Coghi, P.; Yang, L.J.; Ng, J.P.L.; Haynes, R.K.; Memo, M.; Gianoncelli, A.; Wong, V.K.W.; Ribaudo, G. A Drug Repurposing Approach for Antimalarials Interfering with SARS-CoV-2 Spike Protein Receptor Binding Domain (RBD) and Human Angiotensin-Converting Enzyme 2 (ACE2). *Pharmaceuticals* **2021**, *14*, 954. [CrossRef]

21. Tiwari, M.K.; Coghi, P.; Agarwal, P.; Shyamlal, R.B.K.; Yadav, L.; Sharma, R.; Yadav, D.K.; Sahal, D.; Wong, V.K.W.; Chaudhary, S. Design, Synthesis, Structure-Activity Relationship and Docking Studies of Novel Functionalized Arylvinyl-1,2,4-Trioxanes as Potent Antiplasmodial as well as Anticancer Agents. *ChemMedChem* **2020**, *15*, 1216–1228. [CrossRef] [PubMed]

22. Daina, A.; Michielin, O.; Zoete, V. SwissADME: A free web tool to evaluate pharmacokinetics, drug-likeness and medicinal chemistry friendliness of small molecules. *Sci. Rep.* **2017**, *3*, 42717. [CrossRef] [PubMed]

23. Ertl, P.; Rohde, B.; Selzer, P. Fast calculation of molecular polar surface area as a sum of fragment-based contributions and its application tothe prediction of drug transport properties. *J. Med. Chem.* **2000**, *43*, 3714–3717. [CrossRef] [PubMed]